

Atomic structure of the Si(111)($\sqrt{3} \times \sqrt{3}$)R 30°-Ag surface

J. F. Jia, R. G. Zhao, and W. S. Yang

Department of Physics, Peking University, Beijing 100871, China

(Received 12 March 1992; revised manuscript received 26 July 1993)

In the present work, the atomic structure of the Si(111)($\sqrt{3} \times \sqrt{3}$)R 30°-Ag surface is investigated with the quasikinematic low-energy electron-diffraction approach in conjunction with the constant-momentum-transfer-averaging technique. Our results support the honeycomb-chained-triangle model. The topmost layer of the model consists of Ag atoms arranged as “honeycomb chained trimers.” Below the Ag layer is a Si-trimer layer and then bulklike Si double layers follow. In the optimized model of this work the $\sqrt{3} \times \sqrt{3}$ reconstruction extends down to the fifth Si layer, and there is an oscillatory multilayer relaxation in the selva region. We give all structural parameters of the model.

I. INTRODUCTION

In the last 25 years a great many works have been published on the atomic structure of the Si(111)($\sqrt{3} \times \sqrt{3}$)R 30°-Ag surface.^{1–48} In these works almost all of the surface-sensitive techniques, including Auger-electron spectroscopy (AES),^{2–5,12,13,37} low-energy electron diffraction (LEED),^{6,29} reflection high-energy electron diffraction,^{10,34} x-ray diffraction (XD),^{24,32,43} x-ray photoelectron diffraction,^{8,16,40} transmission electron diffraction,⁴⁷ ion-scattering spectroscopy (ISS),^{5,31} impact-collision ion-scattering spectroscopy (ICISS),^{14,22,33,35,39,45} high-energy ion channeling,^{25,38} x-ray standing wave (XSW),⁴² scanning tunneling microscopy (STM),^{17,18,20,48} photoelectron spectroscopy,^{7,19,30,41} inverse photoelectron spectroscopy,¹⁵ surface extended x-ray-absorption fine structure,¹¹ and high-resolution reflection electron microscopy⁴⁷ together with some theoretical efforts^{26–28,46} have been used to study the surface. As a result, many plausible structural mod-

els of the surface, including the simple honeycomb (HC) model,^{9,14,17,20} missing-top-layer (MTL) model,^{8,18,19,20,40} embedded-honeycomb (EHC) model,^{5,6,11} centered hexagon (CH) model,⁴ atop trimer (T) model,² substitutional trimer (ST) model,^{10,13,18,22,23} silicon-adatom-vacancy (SAV) model,³¹ honeycomb-chained-triangle (HCT) model,^{24,43,45,46} and the silver-honeycomb-chained-triangle (SHCT) model,^{32,47} have been proposed. For the top and side views of all these models see Ref. 39.

Despite the fact that the details of the atomic structure of $\sqrt{3}$ -Ag is still a pending problem, after 25 years of intensive investigation,^{1–48} many features of the surface have gradually been disclosed. In Table I we list these features along with the proposed models and summarize which of the features each of the models is compatible with. It should be clear that HCT is the only valid model for this surface, even though some of the features may be questionable. In fact, the majority of the works published recently directly support the HCT model^{24,43,45,46} or similar models.^{32–34,39,47}

TABLE I. Survey of the compatibilities of the proposed models with the established features of the Si(111)($\sqrt{3} \times \sqrt{3}$)R 30°-Ag surface. + denotes compatible; – denotes incompatible.

	HC	MTL	EHC	CH	T	ST	SAV	HCT	SHCT
Each unit cell contains 3 Ag atoms (Refs. 2, 4, 24, and 31)	–	–	–	+	+	+	+	+	+
The Ag atoms reside above the first Si layer (Refs. 14, 35, and 45)	+	–	–	+	+	–	–	+	–
The Ag atoms are laterally displaced away from bulk Si positions (Ref. 42)	–	–	–	–	+	+	+	+	+
The Ag-Ag neighbor interaction is weak (Refs. 36 and 41)	+	+	+	+	–	–	–	+	+
The surface is highly reconstructed (Refs. 25, 31, and 38)	–	+	+	–	–	+	+	+	+
There is only one type of surface Si atom (Ref. 19)	+	+	–	+	+	–	–	+	–
The surface is semiconducting (Refs. 7, 15, 18, and 30)	– ^a	– ^a				– ^a		+ ^a	– ^a

^aReference 46.

Intuitively, one might think that the HCT model is incompatible with the STM images.^{17,18} Actually, recent theoretical work⁴⁶ and STM image calculations⁴⁸ indicate that the HCT model is not only compatible with the bias-voltage dependence of the STM images,^{17,18} but is also in agreement with the registry determined by STM.²⁰

Thus, we feel that it is the right time for the LEED contribution to be considered. Since we have recently proposed the quasikinematic LEED/constant-momentum-transfer-averaging (QKLEED/CMTA) method,⁴⁹ where the QKLEED calculations are combined with the CMTA technique,^{50,51} and have proved its capability in solving atomic structure of complex surfaces, in the present work we employ this method. Through a thorough optimization of the structural parameters we obtained the optimized HCT model, which consists of a honeycomb-chained-triangle Ag layer and five $\sqrt{3} \times \sqrt{3}$ reconstructed Si layers as well as a Si bulk. In addition, we show that even the model most similar to SHCT,^{32,47} i.e., the HCT model with a silicon honeycomb on top of it, is confidently ruled out.

II. EXPERIMENT

The experiments were performed on a UHV system (Riber) consisting of a sample preparation chamber and a main chamber. The latter was equipped with LEED, AES, and electron-energy-loss spectroscopy and its base pressure was in the $4\text{--}8 \times 10^{-11}$ -torr range. The sample was a Si wafer with a size of $8 \times 12 \times 0.5$ mm³ and its orientation was measured with a precision better than 0.5° . After Ar⁺ bombardment, heating (1100°C for 5 min) and annealing (850°C for 10 min) a very sharp 7×7 LEED pattern was routinely obtained. Ag deposition was carried out in the sample preparation chamber. During the deposition the pressure was maintained at better than 7×10^{-10} torr and the sample was kept at room temperature. The $\sqrt{3}$ -Ag structure was formed by depositing about 1 monolayer (ML) (7.8×10^{14} atoms/cm²) of Ag at a rate of about 0.25 ML/min and subsequent annealing at about 500°C for a couple of minutes. Such surfaces were very clean and exhibited excellent $\sqrt{3} \times \sqrt{3}$ LEED patterns.

The LEED I-E curves were collected with the tv-camera-computer system. The sample manipulator allows the incidence angle to vary within $0^\circ\text{--}21^\circ$ and the azimuthal angle from 0° to 360° , which are large enough to effectively reduce the influences of multiple scattering, provided the number of I-E spectra involved in a CMTA curve and the incidence geometries of these spectra are carefully arranged in the way suggested previously.⁴⁹ From each diffraction beam more than one CMTA curve with different incidence geometries were measured, and those CMTA curves were in good agreement with one another. This procedure ensures that the CMTA curves are indeed reliable and that the influences of multiple scattering on them have essentially been eliminated.

III. QKLEED CALCULATIONS

LEED is a particularly useful technique for determining the structural details of surfaces because it is sensitive

to the structure of not only the top atomic layer but also several layers in the selvage region.^{51–54} However, the full dynamic LEED calculations are so time consuming^{51,54} that they are very difficult to use to thoroughly optimize all structural parameters of complex models. In this respect, the newly proposed QKLEED/CMTA method⁴⁹ is much more useful. Since in the method the mean complex atomic scattering factor (MCASF) is introduced,⁴⁹ it is valid for surfaces consisting of more than one element. In fact, by means of the QKLEED/CMTA we have obtained a model of the Si(111)($\sqrt{3} \times \sqrt{3}$)R 30°-Al surface, which is almost identical to the one obtained with full dynamic LEED calculations.⁵⁵ Therefore, the QKLEED/CMTA method is suitable for determining the atomic structure of the $\sqrt{3}$ -Ag surface.

The phase shifts of Ag and Si used for calculating the MCASF's were taken from Ref. 52 and its related LEED package. For both Ag and Si, five phase shifts were used in the calculations. Because there are as many as 14 structural parameters and each of them may vary within

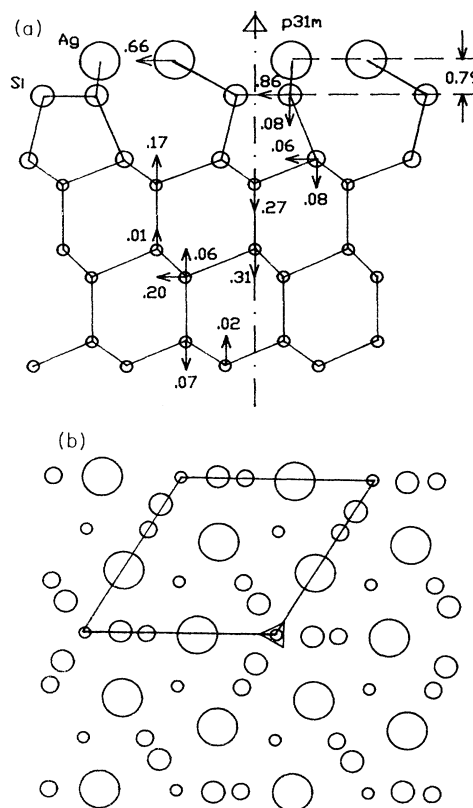


FIG. 1. (a) Side view of the HCT model with a $p31m$ symmetry, showing all optimized structural parameters of this work. The arrows attached to an atom, which all lie on the plane of the figure, show the direction of the atomic shifts from the bulk position of the atom, while the nearby numbers represent the amount in Å. The atomic shifts of these atoms without arrows can be found according to the $p31m$ symmetry of the model. The vertical distance between the Ag layer and the first Si layer is 0.79 Å. (b) Top view of the model with a $\sqrt{3} \times \sqrt{3}$ unit cell outlined.

TABLE II. Comparison of the structural parameters of the present optimized HCT model with x-ray diffraction (Refs. 32 and 43), low-energy ion scattering (Ref. 45), and first-principles total-energy calculation (Ref. 46) results. The $z\text{-Ag}$ and $z\text{-Si}$ are the vertical distances of the Ag and Si trimer layers above the first Si double layer. Units are in Å.

	XD (Ref. 43)	XD (Ref. 32)	ISS (Ref. 45)	Theory (Ref. 46)	KLEED
Ag-Ag	.507	4.95	5.1	4.95	4.98
	3.39	3.43	3.43	3.45	3.42
Ag-Si	2.68	2.63	2.61	2.60	2.61
	2.54	2.57	2.58	2.54	2.54
Si-Si	2.30	2.32	2.30	2.51	2.35
$z\text{-Si}$	2.1 ± 0.2	2.26	2.23	2.30	2.35
$z\text{-Ag}$	2.95 ± 0.1	3.05 (Ref. 42)	2.98	3.15	3.14

a wide range, to reduce the risk of landing on local minima rather than the global minimum, we employed the simulated annealing approach⁵⁶ and other optimization skills. Throughout the work, the Van Hove–Tong r factor R_{vht} (Ref. 57) was used as the criterion for the agreement between the calculated and experimental curves. The calculations were carried out with a personal computer of 80386 with a coprocessor of 80387.

IV. RESULTS AND DISCUSSION

The HCT model, according to Refs. 43, 45, and 46, is shown in Fig. 1. In each $\sqrt{3} \times \sqrt{3}$ unit cell there are three Ag atoms arranged as “honeycomb-chained trimers” lying above the first Si layer which is a trimerized

missing top layer. As the $\sqrt{3}\text{-Ag}$ surface has the symmetry of $p31m$,⁴⁷ the Si trimer is not twisted as in Ref. 34. The topmost five Si layers are $\sqrt{3} \times \sqrt{3}$ reconstructed as shown in the figure. The surface relaxation extends to the seventh silicon layer, and the bulk silicon starts from the eighth.

To avoid being trapped at local minima, in addition to using the simulated annealing scheme, we also started the optimization processes from several significantly different structures of the HCT model. However, the very similar model parameters were always reached. For each parameter the difference was not larger than 0.03 Å, indicating that the local-minimum problem was indeed solved in the work. All 14 structural parameters of the optimized

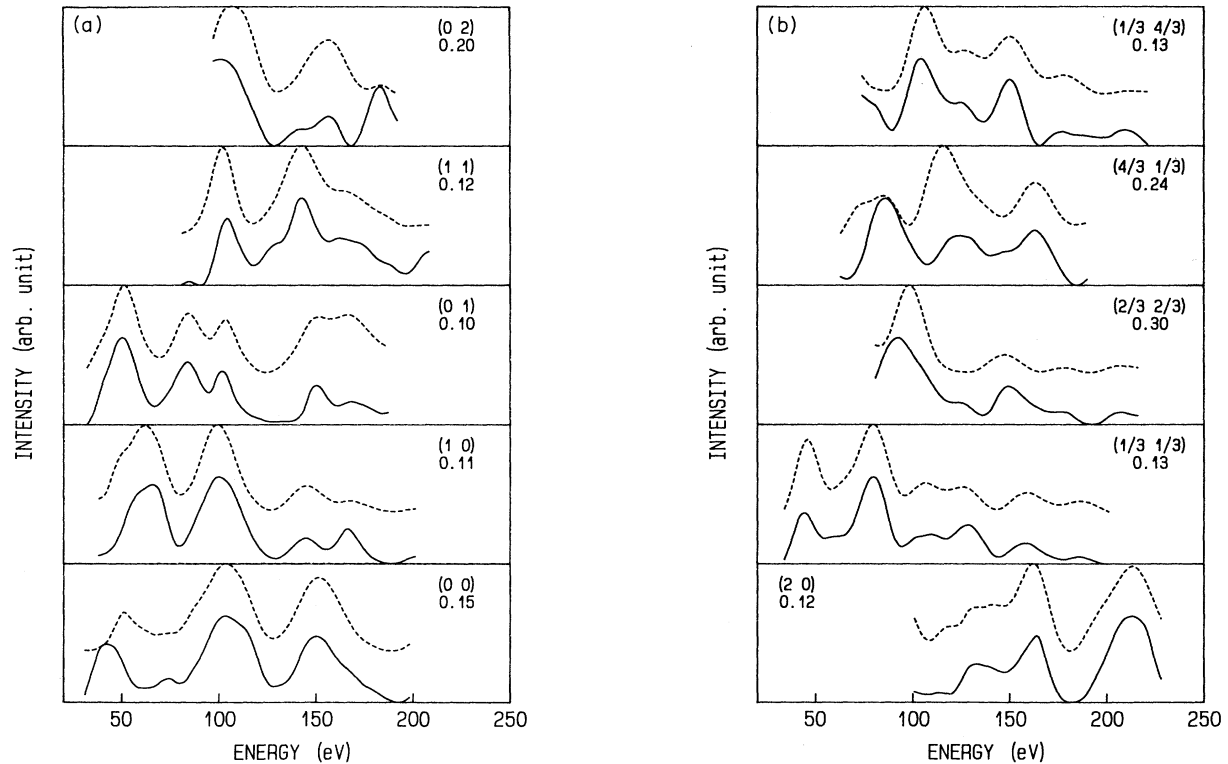


FIG. 2. Comparison of the QKLEED intensity curves (solid) calculated from the optimized HCT model with their experimental CMTA counterparts (dashed). To facilitate optimization of the inner potential, the CMTA curves have been converted to the I-E form of normal incidence (Ref. 49). Shown also in boxes are beam index and beam R_{vht} . The total R_{vht} of the ten beams is 0.16.

TABLE III. Mean-layer spacings of the present optimized HCT model. D_{Ag} is the spacing between the Ag and Si trimer layers, and $D1$ through $D8$ are the first through the eighth Si-Si layer spacings, respectively. Units are in Å.

	D_{Ag}	$D1$	$D2$	$D3$	$D4$	$D5$	$D6$	$D7$	$D8$
Mean-layer spacing	0.79	2.35	0.68	2.47	0.63	2.48	0.69	2.36	0.78

HCT model are shown in Fig. 1(a). The Si-Si bond lengths of the model are all within 6% of the bulk value (2.35 Å). The inner potential is 12.5 eV, and the electron mean free path is 4.5 Å. The total R_{vht} of ten beams is 0.16, indicating an excellent agreement. The experimental CMTA intensity curves (six integral- and four fractional-order beams) and their QKLEED counterparts calculated from the model are shown in Fig. 2.

In Table II our structural parameters are compared with those reported recently in XD (Refs. 32 and 43) and ICISS (Ref. 45) experiments, as well as in first-principles total-energy calculations.⁴⁶ As one can see, our structural parameters match their counterparts of the first-principles calculations excellently with only one exception: the silicon trimer bond length is 2.35 Å in our work as opposed to 2.51 Å in the theoretical work.⁴⁶ However, our value is very close to that of the experimental works.^{32,43,45} Therefore, we suppose that the theoretical value is probably a bit too large.

In a recent x-ray standing-wave experiment it was determined that the Ag layer is located in one plane at a height of 3.44 ± 0.02 Å above the center of the extrapolated bulk Si(111) bilayer.⁴² In our model the corresponding value is 3.45 Å, which is in excellent agreement with the XSW experimental value.

Before the present work only those data listed in Table II were determined for the HCT model,^{24,43,43,45,46} although it has been known that the $\sqrt{3}$ -Ag surface is highly reconstructed or the $\sqrt{3} \times \sqrt{3}$ reconstruction extends down to the deeper Si layers.^{25,31,38} In the present work, the atomic positions of the subsurface Si atoms are determined for the first time (some of them had been estimated by Keating-type energy-minimization calculations⁴⁵). In addition, from the mean-layer spacings listed in Table III one can clearly see that there is an oscillatory multilayer relaxation in the selvage. Of course, the error bar on interlayer spacing of the deeper layers must be quite large. However, qualitatively, there should be no doubt about the existence of the oscillatory multilayer relaxation, since, starting with the significantly different structures of the HCT model, very similar oscillatory multilayer relaxations (the maximum difference of the sixth Si-Si layer spacings ≤ 0.06 Å) resulted. For the $\sqrt{3}$ -Ag surface this

is a phenomenon which had never been reported before. In fact, oscillatory multilayer relaxations have been reported as existing in several clean Si surfaces^{58–60} as well as in the Si(111)($\sqrt{3} \times \sqrt{3}$)R 30°-Al surface;⁴⁹ thus, it seems to be a general phenomenon for silicon surfaces even though its mechanism is as yet unknown.

In order to see if other proposed models could be ruled out by LEED with confidence, we have tested the SHCT model^{32,47} which is very similar to the HCT. By using exactly the same procedure as that used for the HCT model, the best R_{vht} of the SHCT model was only 0.22. Even worse was that to get this R_{vht} many bond lengths in this optimized model had to be physically unfeasible, otherwise the R_{vht} would be worse than 0.22. Consequently, the SHCT and, naturally, the other proposed models should be ruled out.

V. SUMMARY

Based on a general review on the current status of the investigation of the Si(111)($\sqrt{3} \times \sqrt{3}$)R 30°-Ag surface atomic structure by means of the newly proposed QKLEED/CMTA method, we have ruled out all models previously proposed for this surface except the HCT and have obtained the optimized HCT model which has top-most few layers essentially identical to the HCT-1 model of a recent theoretical work⁴⁶ and a selvage with an oscillatory multilayer relaxation that had never been reported before.

The success of the QKLEED/CMTA method in determining the structural parameters of a complex surface that had never before been determined by full dynamic LEED analysis is a strong indication of the applicability of the method for surface determinations.

ACKNOWLEDGMENT

We thank Dr. M. A. Van Hove for providing the LEED package from which the phase-shift data were taken. This work was supported by the National Natural Science Foundation of China and the Doctoral Program Foundation of the Institute of Higher Education of China.

¹K. Spiegel, Surf. Sci. 7, 125 (1967).

²F. Wehking, H. Beckermann, and R. Niedermayer, Surf. Sci. 71, 364 (1978).

³G. Le Lay, M. Manneville, and R. Kern, Surf. Sci. 72, 405 (1978).

⁴G. Le Lay, A. Chauvet, M. Manneville, and R. Kern, Appl. Surf. Sci. 9, 190 (1981).

⁵M. Saitoh, F. Shoji, K. Oura, and T. Hanawa, Surf. Sci. 112, 306 (1981).

⁶Y. Terada, T. Yoshizuka, K. Oura, and T. Hanawa, Surf. Sci. 114, 165 (1982).

⁷T. Yokotsuka, S. Kono, S. Suzuki, and T. Sagawa, Surf. Sci. 127, 35 (1983).

⁸S. Kono, H. Sakurai, K. Higashiyama, and T. Sagawa, Surf.

- Sci. **130**, L299 (1983).
- ⁹G. Le Lay, Surf. Sci. **132**, 169 (1983).
- ¹⁰Y. Horio and A. Ichimiya, Surf. Sci. **133**, 393 (1983).
- ¹¹J. Stohr, R. Jaeger, G. Rossi, T. Kendelewicz, and I. Lindau, Surf. Sci. **134**, 813 (1983).
- ¹²M. Hanbucken, M. Futamoto, and J. A. Venables, Surf. Sci. **147**, 433 (1984).
- ¹³Y. Horio and A. Ichimiya, Surf. Sci. **164**, 589 (1985).
- ¹⁴M. Aono, R. Souda, C. Oshima, and Y. Ishizawa, in *The Structure of Surfaces*, edited by M. A. Van Hove and S. Y. Tong (Springer-Verlag, Berlin, 1985), p. 187.
- ¹⁵J. M. Nicholls, F. Salvan, and B. Reihl, Phys. Rev. B **34**, 2945 (1986).
- ¹⁶S. Kono, K. Higashiyama, and T. Sagawa, Surf. Sci. **165**, 21 (1986).
- ¹⁷R. J. Wilson and S. Chaing, Phys. Rev. Lett. **58**, 369 (1987).
- ¹⁸E. J. van Loenen, J. E. Demuth, R. M. Tromp, and R. J. Hamers, Phys. Rev. Lett. **58**, 373 (1987).
- ¹⁹S. Kono, K. Higashiyama, T. Kinoshita, T. Miyahara, H. Kato, H. Ohsawa, Y. Enta, F. Maeda, and Y. Yaegashi, Phys. Rev. Lett. **58**, 1555 (1987).
- ²⁰R. J. Wilson and S. Chaing, Phys. Rev. Lett. **59**, 2329 (1987).
- ²¹S. Hasegawa, H. Daimon, and S. Ino, Surf. Sci. **186**, 138 (1987).
- ²²T. L. Porter, C. S. Chang, and I. S. T. Tsong, Phys. Rev. Lett. **60**, 1739 (1988).
- ²³J. E. Demuth, E. J. van Loenen, R. M. Tromp, and R. J. Hamers, J. Vac. Sci. Technol. B **6**, 18 (1988).
- ²⁴T. Takahashi, S. Nakatani, N. Okamoto, T. Ichikawa, and S. Kikuta, Jpn. J. Appl. Phys. **27**, L753 (1988).
- ²⁵K. Oura, M. Watamori, F. Shoji, and T. Hanawa, Phys. Rev. B **38**, 10 146 (1988).
- ²⁶Q. Q. Zheng and Z. Zeng, Surf. Sci. **195**, L173 (1988).
- ²⁷S. H. Chou, A. Freeman, S. Grigoras, T. M. Gentle, B. Delley, and E. Wimmer, J. Chem. Phys. **89**, 5177 (1988).
- ²⁸C. T. Chan and K. M. Ho, Surf. Sci. **217**, 403 (1989).
- ²⁹W. C. Fan, A. Ignatiev, H. Huang, and S. Y. Tong, Phys. Rev. Lett. **62**, 1516 (1989).
- ³⁰L. S. O. Johansson, E. Landemark, C. J. Karlsson, and R. I. G. Uhberg, Phys. Rev. Lett. **63**, 2092 (1989).
- ³¹M. Copel and R. M. Tromp, Phys. Rev. B **39**, 12 688 (1989).
- ³²E. Vlieg, A. W. van der Gon, J. F. van der Veen, J. E. MacDonald, and C. Norris, Surf. Sci. **209**, 100 (1989).
- ³³R. S. Williams, R. S. Daley, J. H. Huang, and R. M. Charatan, Appl. Surf. Sci. **41/42**, 70 (1989).
- ³⁴A. Ichimiya, S. Kohomoto, T. Fujii, and Y. Horio, Appl. Surf. Sci. **41/42**, 82 (1989).
- ³⁵K. Sumitomo, K. Tanaka, Y. Izawa, I. Katayama, F. Shoji, K. Oura, and T. Hanawa, Appl. Surf. Sci. **41/42**, 112 (1989).
- ³⁶K. Markert, P. Pervan, W. Heichler, and K. Wandelt, J. Vac. Sci. Technol. A **7**, 2873 (1989).
- ³⁷S. Kono, T. Abukawa, N. Nakamura, and K. Anno, Jpn. J. Appl. Phys. **28**, L1278 (1989).
- ³⁸M. Watamori, F. Shoji, T. Hanawa, and K. Oura, Surf. Sci. **226**, 77 (1990).
- ³⁹R. S. Daley, R. M. Charatan, and R. S. Williams, Surf. Sci. **240**, 136 (1990).
- ⁴⁰E. L. Bullock, G. S. Herman, M. Yamada, D. J. Friedman, and C. S. Fadley, Phys. Rev. B **41**, 1703 (1990).
- ⁴¹B. Vogt, B. Schmiedeskamp, and U. Heinzmann, Phys. Rev. B **42**, 9267 (1990).
- ⁴²E. Vlieg, E. Fontes, and J. K. Patel, Phys. Rev. B **43**, 7185 (1991).
- ⁴³T. Takahashi, S. Nakatani, N. Okamoto, T. Ishikawa, and S. Kikuta, Surf. Sci. **242**, 54 (1991).
- ⁴⁴S. Y. Tong and H. Huang, Surf. Sci. Lett. **243**, L46 (1991).
- ⁴⁵M. Katayama, R. S. Williams, M. Kato, E. Nomura, and M. Aono, Phys. Rev. Lett. **66**, 2762 (1991).
- ⁴⁶Y. G. Ding, C. T. Chan, and K. M. Ho, Phys. Rev. Lett. **67**, 1454 (1991).
- ⁴⁷K. Takayanagi, in *The Structure of Surfaces III*, edited by S. Y. Tong, M. A. Van Hove, K. Takayanagi, and X. D. Xie (Springer-Verlag, Berlin, 1991), p. 227.
- ⁴⁸S. Watanabe, M. Aono, and M. Tsukada, Phys. Rev. B **44**, 8330 (1991).
- ⁴⁹J. F. Jia, R. G. Zhao, and W. S. Yang, Phys. Rev. **48**, 18101 (1993).
- ⁵⁰M. G. Lagally, T. C. Ngoc, and M. B. Webb, Phys. Rev. Lett. **26**, 1557 (1971).
- ⁵¹J. B. Pendry, *Low-Energy Electron Diffraction* (Academic, New York, 1974).
- ⁵²M. A. Van Hove and S. Y. Tong, *Surface Crystallography by Low-Energy Electron Diffraction: Theory, Computation and Structural Results* (Springer-Verlag, Berlin, 1979).
- ⁵³F. Jona, J. A. Strozier, Jr., and W. S. Yang, Rep. Prog. Phys. **45**, 527 (1982).
- ⁵⁴M. A. Van Hove, W. H. Weinberg, and C.-M. Chan, *Low-Energy Electron Diffraction* (Springer-Verlag, Berlin, 1986).
- ⁵⁵H. Huang, S. Y. Tong, W. S. Yang, H. D. Shih, and F. Jona, Phys. Rev. B **42**, 7483 (1990).
- ⁵⁶W. H. Press, B. P. Flannery, S. A. Teukolsky, and W. T. Vetterling, *Numerical Recipes* (Cambridge University Press, Cambridge, MA, 1986), Chap. 10; S. Kirkpatrick, C. D. Gelat, Jr., and M. P. Vecchi, Science **220**, 671 (1983).
- ⁵⁷M. A. Van Hove, S. Y. Tong, and M. H. Elconin, Surf. Sci. **64**, 85 (1977).
- ⁵⁸W. S. Yang and R. G. Zhao, Phys. Rev. B **30**, 6016 (1984).
- ⁵⁹R. G. Zhao and W. S. Yang, Phys. Rev. B **33**, 6780 (1986).
- ⁶⁰R. G. Zhao, J. F. Jia, Y. F. Li, and W. S. Yang, in *The Structure of Surfaces III* (Ref. 47), p. 517.